

Zeeman splitting in single-electron transport through a few-electron quantum dot

Toshimasa Fujisawa,^{1,2,3,*} Gou Shinkai,^{1,2} and Toshiaki Hayashi¹

¹*NTT Basic Research Laboratories, NTT Corporation, 3-1 Morinosato-Wakamiya, Atsugi, 243-0198, Japan*

²*Department of Physics, Tokyo Institute of Technology, 2-12-1 Ookayama, Meguro-ku, Tokyo, 152-8551, Japan*

³*SORST-JST, 4-1-8 Honmachi, Kawaguchi, 331-0012, Japan*

(Received 17 April 2007; revised manuscript received 8 June 2007; published 27 July 2007)

Single-electron transport through a few-electron quantum dot is investigated under in-plane and perpendicular magnetic fields. Zeeman splitting always appears as two conductance peaks, whose conditions depend on whether the total spin is raised or lowered by single-electron tunneling. The total spin of the ground state can be identified by consecutively investigating the Zeeman splitting from a known spin state. Zeeman splitting for some excited states is also discussed.

DOI: [10.1103/PhysRevB.76.041302](https://doi.org/10.1103/PhysRevB.76.041302)

PACS number(s): 73.23.Hk, 73.21.La

Many-body electronic states in a few-electron quantum dot can be characterized by the number of electrons, N , and the total spin, S , in the presence of Coulomb interactions.¹ Actually, spin states have been identified in a well-defined two-dimensional harmonic potential,^{2,3} in a moderate magnetic field where electrons occupy some orbitals associated with the first and second Landau levels,⁴ and in a double quantum dot where electrons occupy spatially separated orbitals.⁵ The assignment of these spin states is based on the orbital characteristics, which strongly depends on the magnetic field or electric potential, but not on the direct spin effect. Spin states can hardly be identified at arbitrary conditions in typical distorted quantum dots. The determination of spin states (spin degeneracy) is important for understanding spin-dependent phenomena⁶ and studying spin-orbit and hyperfine interactions.^{7,8} Here, we propose and demonstrate Zeeman splitting measurement as a way to identify the total spin at least for the ground state. Since spin relaxation time ($>100 \mu\text{s}$) is much longer than the typical characteristic time of the transport (0.1–10 ns),^{9,10} we expect spin-conserved single-electron tunneling, where S and its z component S_z are raised or lowered just by 1/2, otherwise the tunneling is forbidden (spin blockade).^{11,12} The conductance peak for the N -electron ground state splits into *two* (independent of the degeneracy $2S+1$) when S is raised from that for $N-1$ electron number, while no splitting (independent of S) appears when S is lowered. Therefore, as long as the transport is allowed, one can examine the total spin of a few-electron quantum dot by consecutively investigating the appearance of Zeeman splitting starting from the one-electron spin state ($S=1/2$).

Suppose the N -electron ground state has total spin S_0 and the $(N-1)$ -electron ground state has total spin S_{-1} . We have previously demonstrated using pulse-induced tunneling transitions that the transport is allowed only for $S_0=S_{-1}\pm 1/2$.¹² Therefore, our aim is to distinguish whether the total spin is raised or lowered by 1/2. The spin degeneracy for $(N-1)$ - and N -electron systems is lifted in a magnetic field as shown in Fig. 1(a) for the raised case ($S_0=S_{-1}+1/2$) and in Fig. 1(b) for the lowered case ($S_0=S_{-1}-1/2$). The spin selection rule on the z component restricts the possible tunneling transitions to those shown by the arrows. Electrochemical potential for each transition is given by $\mu_{i,j}=E_N(S_i)-E_{N-1}(S_j)$,

where $E_N(S_z)$ is the total energy of the N -electron system with spin z component S_z . Assuming the same Lande g factor for both systems, the electrochemical potential $\mu_{i,j}$ takes μ_+ or μ_- , respectively, for all transitions that raise or lower the spin z component. Here, $E_z\equiv\mu_+-\mu_-$ is the Zeeman energy. Although totally $2S_0+2S_{-1}+1$ transitions are allowed, there are only two electrochemical potentials, μ_+ and μ_- , for the allowed transitions.

We calculated the tunneling current I based on rate equations that describe all possible transitions.¹³ We considered the asymmetric tunneling rate $\Gamma_R=10\Gamma_L$, which is close to our experimental condition described below. The smaller injection rate ($\Gamma_L<\Gamma_R$ at positive V_{DS} in our case) is preferred to investigate N -electron excitation spectra, where conductance peaks appear at the alignment of the source chemical potential μ_S to N -electron electrochemical potentials [see the inset to Fig. 1(c) at $\mu_S=\mu_+$]. The transconductance dI/dV_G is

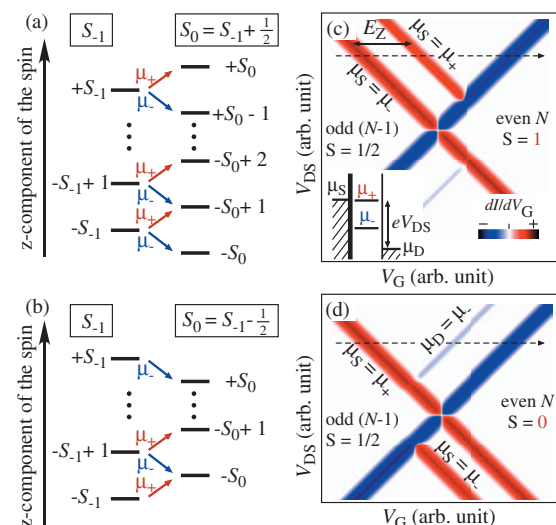


FIG. 1. (Color) (a), (b): Allowed tunneling transitions between Zeeman sublevels in the $N-1$ (left) and N (right) electron systems. Total spin S_0 for the N electron system is raised from total spin S_{-1} for the $N-1$ electron system in (a), but lowered in (b). (c), (d): Calculated transconductance in the V_{DS} - V_G plane, respectively, for the situations in (a) and (b). The inset to (c) is a schematic energy diagram at $\mu_S=\mu_+$ and $V_{DS}>0$.

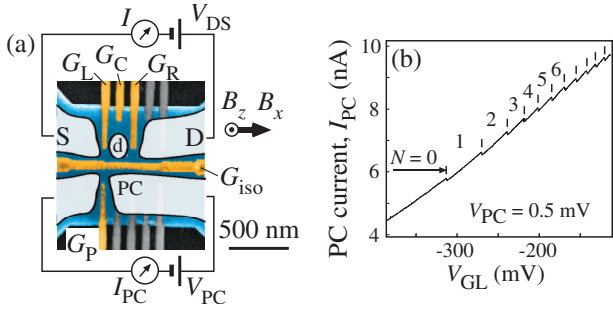


FIG. 2. (Color) (a) Colored SEM image of the sample. (b) PC current for charge measurement on the dot. All measurements were performed in a dilution refrigerator below 100 mK.

plotted as a function of the bias voltage V_{DS} and the gate voltage V_G in Fig. 1(c) for a typical raised case ($S_0=1$ and $S_{-1}=1/2$) and Fig. 1(d) for a typical lowered case ($S_0=0$ and $S_{-1}=1/2$). The Zeeman splitting appears in a different way as clearly shown. When the gate voltage is swept along the dashed line in this situation, conductance peaks for Zeeman splitting appear at $\mu_S=\mu_{\pm}$ only for the raised case. A faint peak at $\mu_D=\mu_{-}$ may be visible for the lowered case (μ_D being the chemical potential of the drain), but can be distinguishable from the condition $\mu_{\pm}=\mu_S$. We use this difference to investigate the total spin of the system.

Figure 2(a) shows a scanning electron micrograph (SEM) of a control device.^{13,14} A single quantum dot [labeled d in Fig. 2(a)] is formed in the upper channel, and the number of electron N in the dot is monitored by the quantum point contact (PC) in the lower channel. The PC conductance ($10\text{--}20\ \mu\text{S}$) in the tunneling regime is influenced by the charge state of the dot.¹³ Figure 2(b) shows the PC current as a function of the gate voltage V_{GL} for the dot, where small jumps correspond to electron depletion from the dot. N can be decreased to 0 by securing the depleting path at least to the drain contact. Observation of the last jump before the depleting path is quenched ensures the zero electron state ($N=0$) in the leftmost region in the figure, and thus we can identify N by counting the jumps. We adjusted all gate voltages to control the dot potential and the two tunneling barriers to allow transport measurement with asymmetric tunnel rates ($\Gamma_R \sim 10\Gamma_L$).⁹ Since the dot current was noisy and thus unreliable for $N < 5$, we had to discuss excitation spectrum for $N=5\text{--}8$. In order to demonstrate the Zeeman splitting at various conditions, we used a two-axis vector magnet to apply perpendicular magnetic field B_z (up to ± 1 T) to change orbital degree of freedom and to apply in-plane magnetic field B_x (up to ± 9 T) to induce Zeeman splitting.

Figure 3 shows B_z dependence of excitation spectra from the $N=5$ system [Fig. 3(d)] to the $N=8$ system [Fig. 3(a)] measured at $B_x=5$ T. Clear Zeeman splitting marked by ‘T’s is observed in all spectra, and the splitting is almost proportional to the magnetic field. For instance, the B_x dependence of the spectra for $N=6$ system is shown in Fig. 3(e) at $B_z=0$ T and Fig. 3(f) at 0.65 T. The observed g factor, $|g|=0.2\text{--}0.3$ depending on the states and fields, is within the variation of the reported values for GaAs quantum dots.^{15–17}

Now, we carefully investigate the appearance of Zeeman

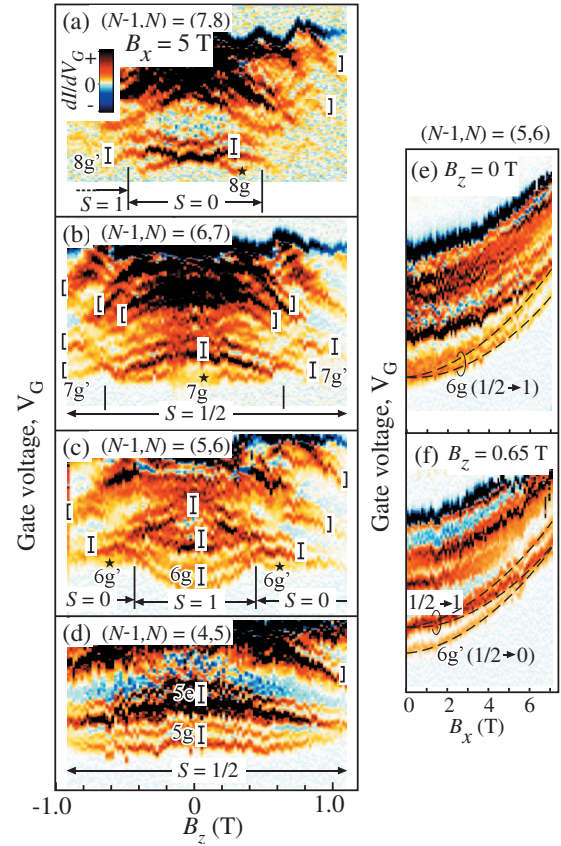


FIG. 3. (Color) Magnetic field dependence of the transconductance dI/dV_G . Gate voltages on G_L , G_C , G_R , and G_{iso} were simultaneously swept along the nominal V_G axis to change the dot potential by keeping the current level 1–100 pA, and dI/dV_G is obtained by numerically differentiating the dot current I at $V_{DS}=1$ mV. (a)–(d): The perpendicular field B_z dependence from (a) $N=8$ down to (d) $N=5$. (e), (f): The in-plane field B_x dependence for $N=6$ at (e) $B_z=0$ T and (f) 0.65 T.

splitting from $N=5$. The ground state [lowest splitting, labeled 5g in Fig. 3(d)] and excited state 5e are clearly resolved, and no level crossing is observed in this magnetic field range. Here, to investigate systems with larger N we assume spin doublet ($S=1/2$) for the $N=5$ ground state, in which four electrons form two spin pairs leaving the last electron unpaired. The next $N=6$ spectra in Fig. 3(c) shows level crossing at $B_z \sim \pm 0.4$ T. In the low field region $|B_z| < 0.4$ T, clear Zeeman splitting is observed [labeled 6g in Figs. 3(c) and 3(e)]. From the above discussions, the appearance of the Zeeman splitting indicates that S is raised by $1/2$, and thus the $N=6$ ground state is a spin triplet ($S=1$) in this region. In contrast, no Zeeman splitting is observed for the ground state at $|B_z| > 0.4$ T [labeled 6g' in Figs. 3(c) and 3(f)], indicating a spin singlet ($S=0$) ground state.

Similarly, the total spin can be determined consecutively for larger electron numbers. The ground state of the $N=7$ spectrum in Fig. 3(b) exhibits no Zeeman splitting at $|B_z| < 0.6$ T (labeled 7g), indicating a spin doublet ($S=1/2$) by lowering the total spin $S=1$ for $N=6$ in the same field region. Zeeman splitting is observed at $|B_z| > 0.6$ T (labeled by 7g'), indicating spin doublet ($S=1/2$) by raising $S=0$ for

$N=6$. The observation suggests $S=1/2$ in the whole region in Fig. 3(b) and orbital level crossing at the field indicated by vertical bars ($B \sim 0.6$ T). The $N=8$ system shown in Fig. 3(a) exhibits no Zeeman splitting in the low-field region (labeled 8g), indicating $S=0$, but does in the high-field region (barely observed at -0.7 – -0.6 T, labeled 8g'), indicating $S=1$. In this way, the total spin of the ground states can be identified consecutively. We started from the $N=5$ system by assuming spin $1/2$ in our example, but this ambiguity can be removed by identifying the total spin from $N=1$, which must be $S=1/2$.

The spin effect in the single electron tunneling regime has already been studied theoretically and experimentally in various systems.^{18,19} Our measurement is closely related to the asymmetric current with respect to the polarity of the bias voltage under asymmetric tunnel barriers.^{20–22} The current is given by the allowed tunneling probabilities and the Clebsch-Gordan coefficients. The ratio of the incoming and outgoing tunneling rates is given by $(2S_0+1)/(2S_{-1}+1)$, which can be used to identify the spin. However, the ratio is often affected by voltage-dependent barriers.^{21,22} The appearance of Zeeman splitting used in our work avoids quantitative measurement and provides an alternate way to determine the spin state.

In general, high spin states appear when the exchange energy exceeds the kinetic energy, which is known as generalized Hund's rule.^{19,23} One would expect there to be a relation between the effective one-electron energy spectrum for the kinetic energy and the two-electron spectrum including the Coulomb interaction. The low energy spectrum of the $N=7$ quantum dot [Fig. 3(b)] can be regarded as for the effective one-electron case, where the orbital crossing (7g and 7g') for the same spin $1/2$ is observed. The triplet ground state (8g') observed in the $N=8$ dot may be associated with the spin-triplet correlation between the orbitals. However, the $N=6$ ground state shows a triplet at zero magnetic field even when the two levels (5g and 5e) for $N=5$ are well separated. Further discussions are out of the scope of the paper, but we believe that, from the Zeeman splitting analysis, we can identify the total spin of the system without knowledge of orbital characteristics.

Next, we discuss Zeeman splitting for excited states. We cannot apply the same rule to the excited states. The two chemical potentials $\mu_+^{(e)}$ and $\mu_-^{(e)}$, which are now for an excited state, appear as Zeeman splitting in the single electron transport regime even if the excited state is a singlet. Actually, all excited states in Fig. 3 exhibit Zeeman splitting. The question then is as follows: Can we determine the spin state of excited states? Figures 4(a) and 4(b) show the calculated transconductance when the total spin of the ground state is lowered ($S_0=S_{-1}-1/2$; $S_0=0$ and $S_{-1}=1/2$). We considered an N -electron excited state with spin singlet for the calculation in Fig. 4(a) and triplet for that in Fig. 4(b). The conductance pattern is more or less the same except inside the circles, where the conductance peak at $\mu_S=\mu_-^{(e)}$ for $\mu_-^{(g)} < \mu_D < \mu_+^{(g)}$ appears only for the triplet excited state. As illustrated in the inset of Fig. 4(a), excitation from the lowest Zeeman sublevel of the $N-1$ electron system to the N -electron singlet excited state is allowed only with electro-

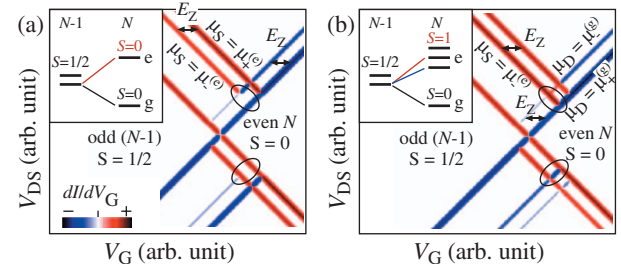


FIG. 4. (Color) Calculated transconductance for the $(N-1)$ -electron doublet ground state and N -electron singlet ground state. The N -electron singlet excited state is considered in (a), and the triplet excited state in (b). The difference is highlighted by circles. The insets show the schematic energy diagrams for the difference.

chemical potential $\mu_+^{(e)}$ (the red line). In contrast, the inset of Fig. 4(b) illustrates that the excitation to the triplet state is allowed with both $\mu_+^{(e)}$ and $\mu_-^{(e)}$ (the red and blue lines, respectively). This difference can be used to identify the excited state. Except for the special case in Fig. 4, however, it may be hard to identify an excited state without a quantitative discussion of the conductance. When the N -electron ground state is raised, the excited state transport can be obtained only when higher Zeeman sublevels of the $N-1$ electron system can be occupied.²⁴ This prevents identifying the excited state.

Figure 5 shows the transconductance profile dI/dV_G in the V_G - V_{DS} plane at (a) $B_x=0$ T and (b) $B_x=5$ T. At zero magnetic field, transconductance peaks (or dips) associated with the ground state (electrochemical potential $\mu^{(g)}$), the first excited states ($\mu^{(6e)}$) for $N=6$, and the excited state ($\mu^{(5e)}$) for $N=5$ are clearly resolved. These peaks in the positive and negative V_{DS} regions are extrapolated to $V_{DS}=0$, where the corresponding potentials are labeled. When the in-plane field is applied [Fig. 5(b)], all electrochemical

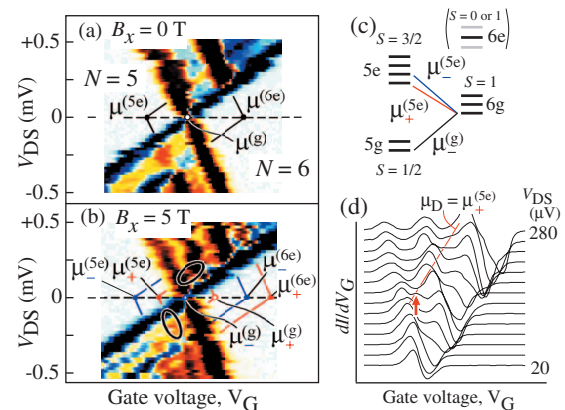


FIG. 5. (Color) Transconductance dI/dV_G in the V_{DS} - V_G plane for $N=6$ at (a) $B_z=0$ T and (b) $B_z=5$ T. The small peak inside the circles in (b) suggests the $S=3/2$ excited state (5e). The corresponding energy diagram is shown in (c). (d) The magnified dI/dV_G traces around the upper circle in (b), highlighting the signal for $\mu_+^{(5e)}$ (marked by the arrow).

potentials exhibit Zeeman splitting (μ_{\pm}) and corresponding transconductance peaks are identified by tracking their in-plane field dependence. The appearance of the Zeeman splitting for the ground state transport is similar to the pattern in Fig. 1(c), which indicates that the total spin of the $N=6$ ground state is raised (spin triplet). In this case, we cannot identify the total spin of the $N=6$ excited state. Instead, the $(N-1)=5$ electron excited state (5e) can be identified by the S_z selection rule. The small peak inside the circles in Fig. 5(b), which is magnified in Fig. 5(d), suggests the excitation from the lowest Zeeman sublevel of $N=6$ to the lowest Zeeman sublevel of $N=5$, as illustrated by the red line in Fig. 5(c). This identifies $S=3/2$ for the $N=5$ excited state. In this way, the spin state of the first excited state can be determined.

In summary, we have proposed and demonstrated a way to identify the total spin of the ground states and some excited states of a few-electron quantum dot by considering single-electron tunneling transitions between Zeeman sublevels. This scheme is useful in identifying level crossing with different spin states. Actually, we see some conductance peaks associated with different S_z and different S [for instance, the singlet state crosses $S_z=1$ of the triplet state at $B_x=7$ T in Fig. 3(f)], where spin-orbit and hyperfine interaction would play an important role in electron dynamics.

We thank Y. Hirayama, T. Ota, and Y. Tokura for valuable comments. This work was supported by the SCOPE from the Ministry of Internal Affairs and Communications of Japan, and by a Grant-in-Aid for Scientific Research from the JSPS.

*Corresponding author. fujisawa@nttbl.jp

¹L. P. Kouwenhoven, D. G. Austing, and S. Tarucha, Rep. Prog. Phys. **64**, 701 (2001).

²S. Tarucha, D. G. Austing, T. Honda, R. J. van der Hage, and L. P. Kouwenhoven, Phys. Rev. Lett. **77**, 3613 (1996).

³L. P. Kouwenhoven, T. H. Oosterkamp, M. W. S. Danoesastro, M. Eto, D. G. Austing, T. Honda, and S. Tarucha, Science **278**, 1788 (1997).

⁴M. Ciorga, A. Wensauer, M. Pioro-Ladriere, M. Korkusinski, J. Kyriakidis, A. S. Sachrajda, and P. Hawrylak, Phys. Rev. Lett. **88**, 256804 (2002).

⁵J. R. Petta, A. C. Johnson, J. M. Taylor, E. A. Laird, A. Yacoby, M. D. Lukin, C. M. Marcus, M. P. Hanson, and A. C. Gossard, Science **309**, 2180 (2005).

⁶M. Pustilnik, L. I. Glazman, and W. Hofstetter, Phys. Rev. B **68**, 161303(R) (2003).

⁷S. Sasaki, T. Fujisawa, T. Hayashi, and Y. Hirayama, Phys. Rev. Lett. **95**, 056803 (2005).

⁸S. I. Erlingsson, Y. V. Nazarov, and V. I. Fal'ko, Phys. Rev. B **64**, 195306 (2001).

⁹T. Fujisawa, Y. Tokura, and Y. Hirayama, Phys. Rev. B **63**, 081304(R) (2001).

¹⁰T. Fujisawa, D. G. Austing, Y. Tokura, Y. Hirayama, and S. Tarucha, Nature (London) **419**, 278 (2002).

¹¹D. Weinmann, W. Hausler, and B. Kramer, Phys. Rev. Lett. **74**, 984 (1995).

¹²T. Fujisawa, D. G. Austing, Y. Tokura, Y. Hirayama, and S. Tarucha, Phys. Rev. Lett. **88**, 236802 (2002).

¹³T. Fujisawa, R. Tomita, T. Hayashi, and Y. Hirayama, Science **314**, 1634 (2006).

¹⁴G. Shinkai, T. Hayashi, Y. Hirayama, and T. Fujisawa, Appl. Phys. Lett. **90**, 103116 (2007).

¹⁵R. M. Potok, J. A. Folk, C. M. Marcus, V. Umansky, M. Hanson, and A. C. Gossard, Phys. Rev. Lett. **91**, 016802 (2003).

¹⁶R. Hanson, B. Witkamp, L. M. K. Vandersypen, L. H. Willems van Beveren, J. M. Elzerman, and L. P. Kouwenhoven, Phys. Rev. Lett. **91**, 196802 (2003).

¹⁷L. H. Willems van Beveren, R. Hanson, I. T. Vink, F. H. L. Koppens, L. P. Kouwenhoven, and L. M. K. Vandersypen, New J. Phys. **7**, 182 (2005).

¹⁸D. Pfannkuche, V. Gudmundsson, and P. A. Maksym, Phys. Rev. B **47**, 2244 (1993).

¹⁹S. Tarucha, D. G. Austing, Y. Tokura, W. G. van der Wiel, and L. P. Kouwenhoven, Phys. Rev. Lett. **84**, 2485 (2000).

²⁰H. Akera, Phys. Rev. B **60**, 10683 (1999).

²¹T. Hayashi, T. Fujisawa, and Y. Hirayama, Phys. Status Solidi B **238**, 262 (2003).

²²D. H. Cobden, M. Bockrath, P. L. McEuen, A. G. Rinzler, and R. E. Smalley, Phys. Rev. Lett. **81**, 681 (1998).

²³G. A. Narvaez and P. Hawrylak, Phys. Rev. B **61**, 13753 (2000).

²⁴O. Agam, N. S. Wingreen, B. L. Altshuler, D. C. Ralph, and M. Tinkham, Phys. Rev. Lett. **78**, 1956 (1997).